

Quantum control of atomic systems by homodyne detection and feedback

Holger F. Hofmann,¹ Günter Mahler,² and Ortwin Hess¹

¹*Institut für Technische Physik, DLR, Pfaffenwaldring 38-40, 70569 Stuttgart, Germany*

²*Institut für Theoretische Physik und Synergetik, Pfaffenwaldring 57, 70550 Stuttgart, Germany*

(Received 28 July 1997; revised manuscript received 30 January 1998)

We investigate the possibilities of preserving and manipulating the coherence of atomic two-level systems by ideal projective homodyne detection and feedback. For this purpose, the photon emission process is described on time scales much shorter than the lifetime of the excited state using a model based on Wigner-Weisskopf theory. The backaction of this emission process is analytically described as a quantum diffusion of the Bloch vector. It is shown that the evolution of the atomic wave function can be controlled completely using the results of homodyne detection. This allows the stabilization of a known quantum state or the creation of coherent states by a feedback mechanism. However, the feedback mechanism can never compensate the dissipative effects of quantum fluctuations even though the coherent state of the system is known at all times. [S1050-2947(98)03406-4]

PACS number(s): 42.50.Lc, 03.65.-w

I. INTRODUCTION

Homodyne detection is a procedure that allows the measurement of a quadrature component of the light field. In quantum optics, it has long been applied to investigating squeezing effects of nonlinear optical systems. In that context it is not necessary to understand the time-resolved properties of the homodyne detection process itself, since the measurement is a time average over many photon emissions from the light field source under investigation. If homodyne detection is to be applied to the observation of individual quantum systems, however, a time-resolved quantum-mechanical treatment of the projective measurements performed by a homodyne detection setup is necessary. Such a description not only helps to improve our understanding of the quantum mechanics of photon emissions, but also provides new methods of controlling the dynamics of quantum systems.

A complete quantum theory of homodyne detection must take into account both the quantization of the field modes and the temporal evolution of the continuous light field entering the detector. The problem of quantization has been addressed in a number of publications [1–4]. An approach to the problem of measuring a system as it evolves in time is presented by Carmichael in [5]. It has been applied to a number of measurement scenarios, including homodyne and heterodyne detection [6,7], as well as to feedback scenarios [9].

In Sec. II of this paper, we present an alternative derivation of this quantum trajectory approach to time-resolved observation of quantum systems by homodyne detection, starting from the projective measurement postulate formulated in [1–4]. In Sec. III this measurement theory is then applied to a description of the spontaneous emission process based on Wigner-Weisskopf theory, which takes into account the field dynamics of the electromagnetic continuum of modes. This derivation provides a shortcut to the formulation of the backaction of the many photon measurements on the two-level atom and illustrates the problems of time resolution and of nonlocality in quantum trajectories, which

are discussed in [5]. Once this control over the information loss induced by spontaneous emission has been established, the observed changes in the atomic wave function can be compensated by feedback. This is investigated in Sec. IV. In Sec. V, the results are interpreted and conclusions are presented.

II. A QUANTUM-MECHANICAL DESCRIPTION OF TIME-RESOLVED HOMODYNE DETECTION

A. Time resolution and projective measurements in the homodyne detection setup

If we know that the linewidth of the emission we wish to observe is much smaller than $1/\tau$, then we can conclude that a time resolution of τ will be sufficient to observe the dynamics of photon emission from the system. We therefore assume that the detectors used provide us with reliable information about the photon numbers that entered each of the detectors during a time interval τ . In fact this is much closer to the experimental situation than the assumption of a continuous measurement in which the arrival of a photon is detected with infinite time resolution. For all time-resolved measurements there is a time window of length τ , which will usually not be shorter than a femtosecond. We can then describe the homodyne detection as a projective measurement on a system of two light field modes of frequency ω_0 . The state to be measured is the product state of the input field state $|\phi\rangle$ and the coherent state $|\alpha\rangle$ produced by the local oscillator. α is the complex field amplitude of the local oscillator mode emitted during the time interval τ . This amplitude is related to the intensity I emitted by the local oscillator via the relation $I = \alpha^* \alpha / \tau$. The measurement base is the photon number base of the symmetric and antisymmetric linear combinations of the input mode and the local oscillator mode, $|n_+, n_-\rangle$. In terms of the input and local oscillator fields, this state may be written as

$$|n_+, n_-\rangle = \frac{1}{\sqrt{n_+! n_-!}} \left(\frac{\hat{a}^\dagger + \hat{b}^\dagger}{\sqrt{2}} \right)^{n_+} \left(\frac{\hat{a}^\dagger - \hat{b}^\dagger}{\sqrt{2}} \right)^{n_-} |\text{vacuum}\rangle, \quad (1)$$

where \hat{a}^\dagger is the creation operator of the local oscillator light field mode ($\langle \alpha | \hat{a}^\dagger = \alpha^* \langle \alpha |$) and \hat{b}^\dagger is the creation operator of the input field.

The effect of this measurement on the input field state $|\phi\rangle$ is a projective measurement on a set of states that is neither orthogonal nor normalized within the subspace of interest. The state $|P(n_+, n_-)\rangle$ projected into by a measurement of n_+ and n_- photons in the detectors is found by forming the scalar product with $\langle \alpha |$ in the subspace of the local oscillator field. Using the fact that $\langle \alpha |$ is an eigenvector of \hat{a}^\dagger , one obtains

$$\begin{aligned} |P(n_+, n_-)\rangle &= \frac{e^{-|\alpha|^2/2}}{\sqrt{n_+!n_-!}} \left(\frac{\alpha^* + \hat{b}^\dagger}{\sqrt{2}} \right)^{n_+} \left(\frac{\alpha^* - \hat{b}^\dagger}{\sqrt{2}} \right)^{n_-} |\text{vacuum}\rangle. \end{aligned} \quad (2)$$

Note that even though this state is not normalized, the probability of a measurement of n_+ and n_- is nevertheless given by

$$p(n_+, n_-) = |\langle \phi | P(n_+, n_-)\rangle|^2. \quad (3)$$

The projection operators associated with these states form a complete probability measure for the subsystem of the input light field. It has been shown that the photon number difference $n_+ - n_-$ corresponds very well to the quadrature component of the input field, which is in phase with the local oscillator if the input field photon number is much smaller than $\alpha^* \alpha$ (see, for example, [3]). Therefore, the classical interpretation of a homodyne detection as a measurement of a quadrature component of the input field also applies to the quantum-mechanical measurement.

B. Application to low-intensity light fields

The light field sources we wish to investigate in the following will usually emit only zero or one photon ($n_{\text{in}} = 0, 1$) during the time interval τ . If the input state is the vacuum state, the measurement probability is given by

$$\begin{aligned} p_{\text{vacuum}}(n_+, n_-) &= |\langle \text{vacuum} | P(n_+, n_-)\rangle|^2 \\ &= \frac{e^{-|\alpha|^2}}{n_+!n_-!} \left(\frac{\alpha^* \alpha}{2} \right)^{(n_+ + n_-)}. \end{aligned} \quad (4)$$

For a fixed sum of photons, $N = n_+ + n_-$, this probability distribution is the binomial distribution, which results from the random scattering of the photons by the beam splitter. For large photon numbers $N \gg 1$, this probability distribution may be approximated by a Gaussian. The probability of measuring the photon number difference $\Delta n = n_+ - n_-$ regardless of the total photon number is then given by

$$p_{\text{vacuum}}(\Delta n) = \frac{1}{\sqrt{2\pi\alpha^*\alpha}} \exp\left[-\frac{\Delta n^2}{2\alpha^*\alpha}\right]. \quad (5)$$

This probability distribution represents the vacuum fluctuations of the in-phase quadrature of the incoming field. In the limit of very strong local oscillator fields, the measured value

of this quadrature corresponding to the photon number difference of Δn is given by $\Delta n/2|\alpha|$, reproducing the expected quantum uncertainty of $1/4$ in the quadrature component.

In the case of weak one photon contributions,

$$|\Phi_\beta\rangle \approx |\text{vacuum}\rangle + \beta |n_{\text{in}} = 1\rangle, \quad (6)$$

the probability distribution is modified only slightly by the contributions linear in β . To simplify the formalism, the nonorthogonal measurement base of the homodyne detection may be reduced to the components lying in the two-dimensional subspace of zero or one photon and the amplitude factor corresponding to the binomial distribution for the vacuum can be approximated by a Gaussian. The resulting measurement base depends only on the photon number difference Δn and is given by

$$\begin{aligned} |P(\Delta n)\rangle &= (2\pi\alpha^*\alpha)^{-1/4} \exp\left[-\frac{\Delta n^2}{4\alpha^*\alpha}\right] \\ &\times \left(|\text{vacuum}\rangle + \frac{\Delta n}{\alpha^*} |n_{\text{in}} = 1\rangle \right). \end{aligned} \quad (7)$$

Note that the weak field condition can be fulfilled for any input field intensity by choosing a time scale τ that is much smaller than the average rate of photons corresponding to the intensity of the input field. Therefore, the simplified projection state $|P(\Delta n)\rangle$ can describe the time evolution of any homodyne detection scenario. Applying Eq. (7) to the weak field state $|\Phi_\beta\rangle$ results in a probability distribution of

$$p_\beta(\Delta n) = \frac{1}{\sqrt{2\pi\alpha^*\alpha}} \exp\left[-\frac{[\Delta n - (\alpha^*\beta + \beta^*\alpha)]^2}{2\alpha^*\alpha}\right]. \quad (8)$$

Effectively, the weak coherent field characterized by β shifts the Gaussian distribution by just the amount expected from classical homodyne detection.

III. QUANTUM DIFFUSION OF A TWO-LEVEL ATOM

A. Description of the emission process

The coherent quantum dynamical evolution of an atomic system interacting with the light field continuum is given by Wigner-Weisskopf theory. The spatiotemporal interpretation of this theory shows that emission processes can be described by a temporal evolution of the following type [10]:

$$\langle E; \text{vacuum} | \Psi(t) \rangle = e^{(-i\omega_0 - \Gamma/2)t}, \quad (9a)$$

$$\langle G; r | \Psi(t) \rangle = \begin{cases} -i \sqrt{\frac{\Gamma}{c}} e^{(\Gamma/2 + i\omega_0)(r/c - t)} & \text{for } 0 < r < ct \\ 0 & \text{otherwise,} \end{cases} \quad (9b)$$

where $|E; \text{vacuum}\rangle$ is the state of the excited atom in the light field vacuum and $|G; r\rangle$ is the state of the ground state

atom with a photon at a distance of r from the atom. Γ is the rate of spontaneous emission.

During a time interval τ , which is much shorter than $1/\Gamma$, the product state of the light field vacuum and an arbitrary linear combination of the excited state $|E\rangle$ and the ground state $|G\rangle$,

$$|\Psi(0)\rangle = c_E|E; \text{vacuum}\rangle + c_G|G; \text{vacuum}\rangle, \quad (10)$$

therefore evolves into an entangled state of the system and the light field, with the light field being in the vacuum state or in a single photon state. The single-photon wave function will be located within a distance of $c\tau$ from the atom. Since the emission has a well-defined frequency and angular dependence, the mode into which the photon has been emitted is a well-defined mode and the total state of atom and field can be written as

$$|\Psi(\tau)\rangle = c_E[1 - (i\omega_0 + \Gamma/2)\tau]|E; \text{vacuum}\rangle + c_G|G; \text{vacuum}\rangle + c_E\sqrt{\Gamma\tau}|G; n_0=1\rangle. \quad (11)$$

The amplitude factor of $\sqrt{\Gamma\tau}$ is found by normalizing the rectangular mode emitted by the system after a time interval of τ . This is done by dividing the amplitude of $\sqrt{\Gamma}/c$ emitted into the spatially continuous one-dimensional field by the amplitude of the normalized rectangular mode of length $c\tau$, which is equal to $\sqrt{1/c\tau}$. Note that the amplitude of the emission depends on the square root of τ , reflecting the linear increase of emission probability with time.

In homodyne detection, the frequency of the local oscillator is also ω_0 . Therefore, it is useful to transform to the interaction picture using the time-dependent transformation

$$|\tilde{E}\rangle = e^{-i\omega_0 t}|E\rangle. \quad (12)$$

This effectively removes the terms oscillating with ω_0 from the system dynamics by describing the phase relation between the excited-state component and the ground-state component of the system state not in terms of an absolute phase but in terms of the phase relative to the local oscillator. Note that heterodyne detection may also be described by this formalism if the time scale τ is chosen so that the detuning $\delta\omega$ between the local oscillator and the system dynamics satisfies the requirement that $\delta\omega\tau \ll 1$. The dynamical evolution of the system phase relative to the local oscillator phase can then be included in the measurement scenario.

The equation for the evolution of the wave function during short time intervals τ is

$$|\Psi(\tau)\rangle = c_E(1 - \Gamma\tau/2)|\tilde{E}; \text{vacuum}\rangle + c_G|G; \text{vacuum}\rangle + c_E\sqrt{\Gamma\tau}|G; n_0=1\rangle. \quad (13)$$

The projection postulate of homodyne detection can now be applied to the light field part of this correlated system-field state, resulting in an effective projection of the state of the atomic system into a state that depends on the measurement result of the homodyne detection.

Although the real physical measurement will take place many time intervals τ later, after the light-field wave func-

tion has traveled the distance to the detectors, it is possible to interpret the measurement as an instantaneous projection on the local light field state, since the light-field signal, once emitted, will not interact with the atom again. This artificial choice of the instant in which the state is projected is consistent with the basic theory of quantum measurement, since it is not possible to distinguish between a projection at the time of a measurement and a projection that anticipates the measurement. It is only our subjective expectation of causality that leads us to prefer placing the collapse after the measurement.

Also the measurement described here is not continuous in the sense discussed in [6,7]. The discrete measurements performed are measurements of properties of the total interval τ . For this reason τ is not written as dt , which would suggest the limit of infinite time resolution. The experimental result corresponding to the situation described here is a series of photon numbers without any zero-photon time intervals separating the time windows of each measurement.

If the wave function is regarded as an epistemological tool describing not physical reality itself but only our knowledge of it, then the projective measurement at the atom is simply an expression of the information gained about the events at the atom, independent of the time at which the information is actually obtained. In a completely relativistic theory of measurement, this epistemological effect of future knowledge on the state of the past must be considered, as was already pointed out by Einstein [11]. The arbitrary subdivision of the flow of time into segments of duration τ is also an epistemological consequence as it represents the time aspect of the space-time measurement base defined by the experimental setup. Information about the atomic system dynamics on shorter time scales is not obtained and cannot be included in the evolution of the system wave function.

B. Influence of the homodyne detection on the system dynamics

For an arbitrary system with known initial wave function, the measurement protocol of repeated homodyne detections provides a complete description of the evolution of the system wave function. In this sense, the method described here is a generalized quantum trajectory approach. However, instead of using a master equation approach, Schrödinger's equation of the system-field interaction is solved and the homodyne detection events are described as projective measurements on the correlated system-field wave function. The detector simulated by this approach is not a single-photon counting device but rather corresponds to a photodiode with a high time resolution. Indeed, the measurement need not resolve single photon counts to achieve a useful precision for predictions about the quantum system.

To investigate the dynamics of the atomic wave function observed by homodyne detection, it is useful to examine the effect of a single projective measurement of photon number difference Δn on an arbitrary system wave function after an emission time segment of τ . Before the projective measurement, the correlated system-field wave function is given by Eq. (13). After the projective measurement of Δn the system is in a pure state described in the interaction picture by

$$\begin{aligned}
|\psi(\tau)\rangle &= \langle P(\Delta n) | \Psi(\tau) \rangle \\
&= (2\pi\alpha^*\alpha)^{-1/4} \exp\left[-\frac{\Delta n^2}{4\alpha^*\alpha}\right] \\
&\quad \times \left[c_E(1-\Gamma\tau/2)|\tilde{E}\rangle + \left(c_G + c_E\sqrt{\Gamma\tau}\frac{\Delta n}{\alpha} \right) |G\rangle \right]. \quad (14)
\end{aligned}$$

The squared length of this state vector is a measure of the probability of measuring (n_+, n_-) . Proceeding as in the derivation of Eq. (8) and assuming that $\Gamma\tau \ll 1$, it is possible to represent the deviation of this probability distribution from the vacuum state distribution by a Gaussian distribution shifted by a term linear in $\sqrt{\Gamma\tau}$:

$$p(\Delta n) \approx \frac{1}{\sqrt{2\pi\alpha^*\alpha}} \exp\left[-\frac{[\Delta n - |\alpha|\sqrt{\Gamma\tau}(c_Ec_G^* + c_E^*c_G)]^2}{2\alpha^*\alpha}\right]. \quad (15)$$

Here and in the following, the phase relation between the local oscillator and the atomic dipole is defined so that it is zero if both c_E and c_G are real and positive. The small deviation from the quantum vacuum case is clearly related to the dipole expectation value of the atomic system. Consequently, they indicate the dipole field emitted by the system. The normalized change in the state of the system is orthogonal to the initial state $|\psi(0)\rangle$ for small changes. It is found by projecting $|\psi(\tau)\rangle$ on the subspace orthogonal to $|\psi(0)\rangle$, normalizing by dividing by the amplitude of the parallel component.

$$|\delta\psi(\tau)\rangle = \frac{|\psi(\tau)\rangle - |\psi(0)\rangle\langle\psi(0)|\psi(\tau)\rangle}{\langle\psi(0)|\psi(\tau)\rangle}. \quad (16)$$

The normalized expression for the system wave function is then given by $|\psi(0)\rangle + |\delta\psi(\tau)\rangle$. Applying the condition that $\Gamma\tau \ll 1$ we neglect all terms above second order in $\sqrt{\Gamma\tau}$. The change of the wave function $|\delta\psi(\tau)\rangle$ within the time interval τ conditioned by the measurement of Δn is then given by

$$\begin{aligned}
|\delta\psi(\tau)\rangle &= -\sqrt{\Gamma\tau}\frac{\Delta n}{|\alpha|}c_E^2(c_G^*|\tilde{E}\rangle - c_E^*|G\rangle) \\
&\quad + \Gamma\tau\frac{\Delta n^2}{\alpha^*\alpha}c_E^3c_G^*(c_G^*|\tilde{E}\rangle - c_E^*|G\rangle) \\
&\quad - \frac{\Gamma\tau}{2}c_Ec_G(c_G^*|\tilde{E}\rangle - c_E^*|G\rangle). \quad (17)
\end{aligned}$$

The dominant effect within one time interval is given by the diffusion term proportional to $\sqrt{\Gamma\tau}\Delta n$. The average of

these diffusion steps is only proportional to $\Gamma\tau$ however, since the expectation value of $\Delta n/\alpha$ is of the order of $\sqrt{\Gamma\tau}$. On the measurement time scale τ , the quantum fluctuations therefore cause a random-walk-type diffusion of the atomic state, just as one would expect from classical noise. However, the length and the phase of the diffusion step are functions of the initial system state. On time scales of $1/\Gamma$, the nonzero average of $\Delta n/\alpha$, the diffusion term proportional to the square of the measurement, and the deterministic drift terms contribute to the change in the system state. All of these terms give rise to a slow drift of the wave function towards the ground state. To illustrate the dependence of the diffusion constant on the state of the atomic system and to identify the drift terms we will now formulate this dependence of these processes in terms of the Bloch vector.

C. Quantum diffusion of the Bloch vector

The dynamics of two-level systems can be visualized using the Bloch vector representation. This three-dimensional vector incorporates the excitation (population inversion), the dipole, and the dipole current of the two level atom as its orthogonal components. When the time-dependent transformation given in Eq. (12) is used, the two components orthogonal to the excitation s_z describe the in-phase and the $(\pi/2)$ out-of-phase components, respectively, of the dipole oscillations relative to the local oscillator:

$$s_x = 2 \operatorname{Re}(\langle\psi|\tilde{E}\rangle\langle G|\psi\rangle), \quad (18a)$$

$$s_y = 2 \operatorname{Im}(\langle\psi|\tilde{E}\rangle\langle G|\psi\rangle), \quad (18b)$$

$$s_z = |\langle\tilde{E}|\psi\rangle|^2 - |\langle G|\psi\rangle|^2. \quad (18c)$$

If α is a real number, s_x is the in-phase component of the atomic dipole and s_y is the out-of-phase component. The diffusion step associated with a measurement result of Δn in terms of the Bloch vector is derived from $|\psi(0)\rangle$ and $|\delta\psi(\tau)\rangle$ by using

$$\delta s_x = 2 \operatorname{Re}[\langle\psi(0)|\tilde{E}\rangle\langle G|\delta\psi(\tau)\rangle + \langle\delta\psi(\tau)|\tilde{E}\rangle\langle G|\psi(0)\rangle], \quad (19a)$$

$$\delta s_y = 2 \operatorname{Im}[\langle\psi(0)|\tilde{E}\rangle\langle G|\delta\psi(\tau)\rangle + \langle\delta\psi(\tau)|\tilde{E}\rangle\langle G|\psi(0)\rangle], \quad (19b)$$

$$\delta s_z = 2 \operatorname{Re}[\langle\psi(0)|\tilde{E}\rangle\langle\tilde{E}|\delta\psi(\tau)\rangle - \langle\psi(0)|G\rangle\langle G|\delta\psi(\tau)\rangle]. \quad (19c)$$

The change in the Bloch vector $\delta\mathbf{s}$ can be expressed in terms of the Bloch vector \mathbf{s} corresponding to $|\psi(0)\rangle$. The result is the diffusion step of the Bloch vector,

$$\begin{pmatrix} \delta s_x \\ \delta s_y \\ \delta s_z \end{pmatrix} = \sqrt{\Gamma\tau}\frac{\Delta n}{|\alpha|} \begin{pmatrix} 1+s_z-s_x^2 \\ -s_xs_y \\ -s_x(1+s_z) \end{pmatrix} - \Gamma\tau\frac{\Delta n^2}{\alpha^*\alpha}s_x \begin{pmatrix} 1+s_z-s_x^2 \\ -s_xs_y \\ -s_x(1+s_z) \end{pmatrix} + \frac{\Gamma\tau}{2}\frac{\Delta n^2}{\alpha^*\alpha}(1+s_z) \begin{pmatrix} s_xs_z \\ s_ys_z \\ s_z^2-1 \end{pmatrix} + \frac{\Gamma\tau}{2} \begin{pmatrix} s_xs_z \\ s_ys_z \\ s_z^2-1 \end{pmatrix}. \quad (20)$$

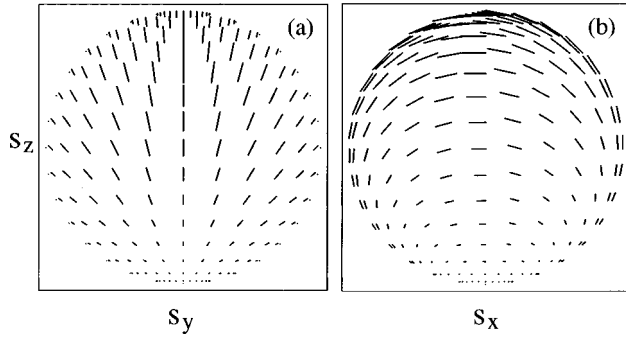


FIG. 1. Visualization of the diffusion step on the Bloch sphere. The diffusion is represented by lines oriented parallel to the direction of the diffusion with a length proportional to the standard deviation of the diffusion step. (a) shows the projection into the (s_y, s_z) plane and (b) the projection into the (s_x, s_z) plane.

As in the case of the state vector representation, the Bloch vector diffusion step is composed of a fast random walk diffusion on the time scale of τ and drift terms on a time scale of $1/\Gamma$. What is more apparent in the Bloch vector representation is the possible separation into phase-sensitive and phase-independent changes.

D. Interpretation of the contributions to the diffusion step

To interpret the diffusion step, it is useful to analyze the separate contributions in more detail. In particular it is helpful to investigate the diffusion step component representing the random walk caused by the fluctuating light field,

$$\begin{pmatrix} \delta s_x \\ \delta s_y \\ \delta s_z \end{pmatrix}_{\text{fluctuation}} = \sqrt{\Gamma} \tau \frac{\Delta n}{|\alpha|} \begin{pmatrix} 1 + s_z - s_x^2 \\ -s_x s_y \\ -s_x(1 + s_z) \end{pmatrix}. \quad (21)$$

Figure 1 illustrates this diffusion on the Bloch sphere. In order to analyze the diffusive motion of the Bloch vector, one may separate the absolute value from the direction of the diffusion. The diffusion constant is then given by

$$\frac{\langle \delta \mathbf{s}^2 \rangle}{\tau} = \Gamma (1 + s_z)^2. \quad (22)$$

The magnitude of the diffusion is therefore independent of the phase relation between the local oscillator and the atomic dipole. It does depend on the excitation of the atom however. It is maximal for the excited state and zero for the ground state, indicating that the ground state will not interact with the field vacuum. The direction of $\delta \mathbf{s}$ is given by

$$\frac{\delta \mathbf{s}}{|\delta \mathbf{s}|} = \frac{1}{1 + s_z} \begin{pmatrix} 1 + s_z - s_x^2 \\ -s_x s_y \\ -s_x(1 + s_z) \end{pmatrix} = \frac{s_y}{\sqrt{s_x^2 + s_y^2}} \hat{\mathbf{e}}_{\perp} + \frac{s_x}{\sqrt{s_x^2 + s_y^2}} \hat{\mathbf{e}}_{\parallel}, \quad (23a)$$

where $\hat{\mathbf{e}}_{\perp}$ is the unit vector perpendicular to both \mathbf{s} and the z axis and $\hat{\mathbf{e}}_{\parallel}$ is the unit vector perpendicular to both \mathbf{s} and $\hat{\mathbf{e}}_{\perp}$.

$$\hat{\mathbf{e}}_{\perp} = \frac{1}{\sqrt{s_x^2 + s_y^2}} \begin{pmatrix} s_y \\ -s_x \\ 0 \end{pmatrix} \quad \text{and} \quad \hat{\mathbf{e}}_{\parallel} = \frac{1}{\sqrt{s_x^2 + s_y^2}} \begin{pmatrix} s_x s_z \\ s_y s_z \\ -s_x^2 - s_y^2 \end{pmatrix}. \quad (23b)$$

As can be seen from these results, a Bloch vector that is in phase with the local oscillator will show random rotations in the (s_x, s_z) plane. A Bloch vector polarized out of phase with the local oscillator by $\pm \pi/2$ ($s_x=0$) will undergo phase diffusion only, with s_z remaining constant. The ratio between the diffusion constant of pure phase diffusion and the diffusion constant of excitation diffusion is given by $(s_y/s_x)^2 = \tan(\phi)^2$, where ϕ is the phase difference between the local oscillator and the dipole oscillations of the atom. Note that a randomly varying classical in-phase field would give rise to Rabi oscillations around s_y with a step length proportional to $\sqrt{1 - s_x^2}$. The properties that only phase diffusion occurs for $s_x=0$ and that the rotations in the $s_y=0$ plane preserve phase are also properties of Rabi rotations induced by classical fields. However, the step length dependence of $1 + s_z$ clearly indicates a difference between the effects of quantum noise and of classical noise.

On a time scale of $1/\Gamma$, the contribution of the random walk is given by the nonvanishing expectation value of the homodyne detection photon number difference. The probability distribution of the measurement results is approximately given by a Gaussian with

$$\left\langle \frac{\Delta n}{|\alpha|} \right\rangle = \sqrt{\Gamma} \tau s_x, \quad (24a)$$

$$\left\langle \frac{\Delta n^2}{\alpha^* \alpha} \right\rangle = 1. \quad (24b)$$

On a time scale of $1/\Gamma$ a large number of measurements will have been performed since $\tau \ll 1/\Gamma$. Therefore, the net change of the system state can be evaluated using these expectation values. The random walk drift is then given by

$$\begin{pmatrix} \langle \delta s_x \rangle \\ \langle \delta s_y \rangle \\ \langle \delta s_z \rangle \end{pmatrix}_{\text{fluctuation}} = \Gamma \tau s_x \begin{pmatrix} 1 + s_z - s_x^2 \\ -s_x s_y \\ -s_x(1 + s_z) \end{pmatrix}. \quad (25)$$

This is exactly compensated by the other phase-sensitive contribution effective on a time scale of $1/\Gamma$,

$$\begin{pmatrix} \langle \delta s_x \rangle \\ \langle \delta s_y \rangle \\ \langle \delta s_z \rangle \end{pmatrix}_{\text{compensation}} = -\Gamma \tau \left\langle \frac{\Delta n^2}{\alpha^* \alpha} \right\rangle s_x \begin{pmatrix} 1 + s_z - s_x^2 \\ -s_x s_y \\ -s_x(1 + s_z) \end{pmatrix}. \quad (26)$$

This compensation has a clear physical reason. The dynamics of the system should only depend on the incoming field. However, the measurement is being performed on the field coming from the atomic system, which is a sum of the fields passing the atom and the dipole field emitted by the atom. Although it is impossible to separate the contributions in a quantum-mechanical measurement, the long term averages can actually be corrected by subtracting the averaged dipole

field contribution from the measured fields. In effect, this leaves only two drift terms that influence the $1/\Gamma$ time scale dynamics.

The drift term that is not dependent on the measurement result Δn is given by

$$\begin{pmatrix} \delta s_x \\ \delta s_y \\ \delta s_z \end{pmatrix}_{\text{dipole}} = \frac{\Gamma \tau}{2} \begin{pmatrix} s_z s_x \\ s_z s_y \\ -s_x^2 - s_y^2 \end{pmatrix}. \quad (27)$$

This term describes a reduction of s_z as a function of $s_x^2 + s_y^2$. Since s_z is the energy expectation value of the atomic system and $s_x^2 + s_y^2$ is the square of the atomic dipole, this process describes a loss of energy corresponding to the emission of radiation from a classical oscillating dipole. It is therefore equivalent to the equations describing superradiance [12,13], as well as to a semiclassical textbook approach to spontaneous emission [14]. Unlike the other terms, this term is entirely free of quantum fluctuation effects. It is completely deterministic and depends only on the expectation values of the atomic system state. It is a fascinating feature of the quantum theoretical formulation of spontaneous emission applied in this investigation that it automatically produces such a semiclassical term from the simple photon emission described by Eq. (11).

The three terms discussed up to this point can be understood in terms of the action of the incoming quantum fluctuations on the system and in terms of the semiclassical emission caused by the dipole oscillations. The fourth term is more difficult to understand since it depends on the quantum fluctuation measurements but is not sensitive to the phase of the local oscillator. It seems to be a mixed effect of dipole emission and quantum fluctuations, possibly related to the quantum fluctuations of the atomic dipole. The contribution of this mixed term to the dynamics is given by

$$\begin{pmatrix} \langle \delta s_x \rangle \\ \langle \delta s_y \rangle \\ \langle \delta s_z \rangle \end{pmatrix}_{\text{mixed}} = \frac{\Gamma \tau}{2} \left\langle \frac{\Delta n^2}{\alpha^* \alpha} \right\rangle (1 + s_z) \begin{pmatrix} s_z s_x \\ s_z s_y \\ -s_x^2 - s_y^2 \end{pmatrix}. \quad (28)$$

The sum of the drift dynamics to be expected on a time scale of $1/\Gamma$ is given by the sum of the dipole contribution and the mixed term. The total drift vectors resulting from this sum are shown in Fig. 2.

E. Contributions to the exponential decay of the average excitation

At first it may seem confusing that a simple spontaneous emission from an isolated atom should give rise to such a complicated variety of dynamical effects. After all, the Bloch vector dynamics of an ensemble of atoms is described by

$$\frac{d}{dt} \begin{pmatrix} \langle s_x \rangle \\ \langle s_y \rangle \\ \langle s_z \rangle \end{pmatrix} = -\Gamma \begin{pmatrix} \langle s_x \rangle / 2 \\ \langle s_y \rangle / 2 \\ \langle s_z \rangle + 1 \end{pmatrix}. \quad (29)$$

If one separates the time derivative of the Bloch vector into a component orthogonal to the Bloch vector and one parallel to

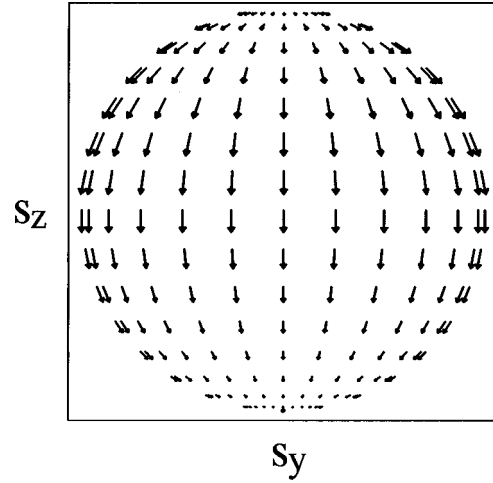


FIG. 2. Total drift on the Bloch sphere projected into the (s_y, s_z) plane. Since the drift is rotationally symmetric around the s_z axis, no extra figure is given for the (s_x, s_z) plane.

it, however, the connection to the dynamics observed in the homodyne detection becomes apparent:

$$\begin{aligned} \frac{d}{dt} \begin{pmatrix} \langle s_x \rangle \\ \langle s_y \rangle \\ \langle s_z \rangle \end{pmatrix} &= \frac{\Gamma}{2} \frac{(2 + \langle s_z \rangle)}{\langle \mathbf{s} \rangle^2} \begin{pmatrix} \langle s_z \rangle \langle s_x \rangle \\ \langle s_z \rangle \langle s_y \rangle \\ \langle s_z \rangle^2 - \langle \mathbf{s} \rangle^2 \end{pmatrix} \\ &\quad - \frac{\Gamma}{2} \frac{(|\langle \mathbf{s} \rangle| + \langle s_z \rangle)^2}{\langle \mathbf{s} \rangle^2} \begin{pmatrix} \langle s_x \rangle \\ \langle s_y \rangle \\ \langle s_z \rangle \end{pmatrix}. \quad (30) \end{aligned}$$

For $|\langle \mathbf{s} \rangle| = 1$, the expected reduction of the length of the Bloch vector is an effect of the diffusion caused by the $\delta \mathbf{s}_{\text{fluctuations}}$ term. Its rate is given by one-half of the diffusion constant $\Gamma(1 + s_z)^2$. The rotation of the Bloch vector is given by the sum of the two drift terms, $\delta \mathbf{s}_{\text{dipole}}$ and $\delta \mathbf{s}_{\text{mixed}}$. For $|\langle \mathbf{s} \rangle| = 1$, the average expected change in s_z can be separated into contributions related to the diffusion of the Bloch vector, to the dipole emission, and to the mixed term,

$$\frac{d}{dt} \langle s_z \rangle = -\Gamma (\langle s_z \rangle + 1) (q_{\text{diffusion}} + q_{\text{dipole}} + q_{\text{mixed}}), \quad (31a)$$

$$q_{\text{diffusion}} = \frac{1}{2} (1 + s_z) s_z, \quad (31b)$$

$$q_{\text{dipole}} = \frac{1}{2} (1 - s_z), \quad (31c)$$

$$q_{\text{mixed}} = \frac{1}{2} (1 - s_z^2). \quad (31d)$$

Figure 3 shows this change in the relative contributions to the exponential decay of the atomic excitation as a function of s_z . For the excited state, $s_z = +1$, the exponential relaxation of s_z is a result of the diffusion of the Bloch vector due to quantum fluctuations, while for states close to the ground state, $s_z \approx -1$, the exponential relaxation to $s_z = -1$ is dominated by the semiclassical dipole emission. For maximally polarized states, $s_z = 0$, the emission contributions of the dipole term and of the mixed term are equally strong, while the diffusion has no effect. Note that for $-1 < s_z < 0$, the diffu-

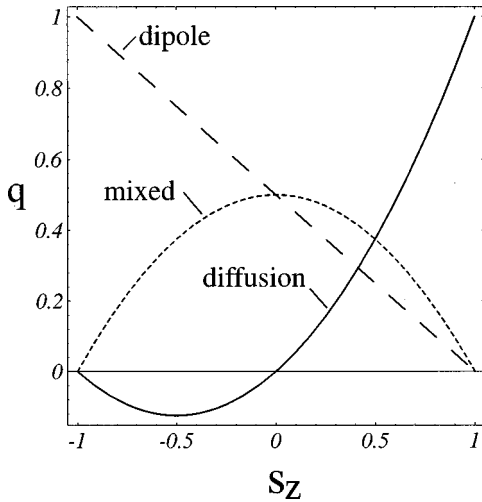


FIG. 3. Relative contributions to the exponential decay of the atomic excitation for $|\langle s \rangle| = 1$.

sion caused by the quantum fluctuations actually tends to excite the atom. However, this effect is compensated by the mixed terms and the dipole emission.

IV. COMPENSATING QUANTUM FLUCTUATIONS BY FEEDBACK

A. Feedback setup

Section III describes the measurement of quantum fluctuations propagating away from an atomic two-level system by homodyne detection and the implications of the measurement for the dynamics of the atomic state. Since maximal knowledge is obtained about the field state, the atomic system state is in a pure state after the measurement. This suggests the possibility of using feedback based on the measurement results as a means to manipulate the quantum state. A general formalism for this procedure based on the master equation approach to quantum trajectories has been presented in [9] and was applied to light fields in an open cavity in [8]. In the following, we will discuss the possibility and the physical problems involved in applying a feedback scheme to the two-level atom.

On a time scale of τ , the homodyne detection does not give any information about the state of the atom. $p(\Delta n)$ is nearly equal to the vacuum probability distribution. The information obtained in a single field measurement is therefore not information about the atomic system itself. Instead, it is information about the quantum fluctuations acting on the system. This sensitivity to the vacuum fluctuations (as opposed to the system state) is ideal for stabilizing quantum states by reversing the effects of the measurement process [15]. If we were dealing with a classical system it would be possible to measure the exact forces involved. A feedback mechanism could then compensate the forces, thereby removing the effects of the incoming noise. In quantum mechanics, however, the quadratures of the light field do not commute. Therefore the force acting on the atomic system can never be known completely. In the balanced homodyne detection setup discussed here we only know the quadrature of the light field, which is in phase with the local oscillator. In a classical system, this lack of information would make

control impossible. In the quantum system, however, we can still achieve perfect control of the atomic wave function.

In order to manipulate the known atomic state the electromagnetic field at the atom may be modified. For example, a resonant coherent driving field may be coupled to the atomic system. In order to ensure that this field has a fixed phase relation with the local oscillator used in the measurement it would be natural to utilize the same coherent light field source in the homodyne detection setup and in the feedback loop. Since the local oscillator field is very strong, only a negligibly small portion needs to be redirected in order to achieve control of the system dynamics. In fact, since the strength of the field expectation value needs to compensate for quantum fluctuations only, the portion of the local oscillator intensity used for this purpose is approximately given by $1/(4\alpha^* \alpha)$. Note that it is possible to add the effect of the Rabi rotations caused by the feedback field and the effects of the quantum fluctuations because the Heisenberg equations of motion for the fully quantum-mechanical field-atom interaction are linear in the field variables. The dynamical effects of the feedback and of the diffusive evolution are therefore separable.

A controllable reflector can be used to coherently manipulate the system depending on the measurement results of the homodyne detection. This feedback modifies the dissipative dynamics of the atomic system. If the delay between emission and feedback is much shorter than $1/\Gamma$, it is possible to compensate the effects of fluctuations on a known system state. Note that this either requires a low decay rate Γ or a very fast feedback loop. In an optical setup a typical unmodified lifetime of nanoseconds would require a feedback loop much shorter than 10 cm in length, so the light field signal can return in time, with the purely optical dissipative photon detectors integrated into this loop.

The effect of a delay time of $\Delta t = m\tau$ between the emission and the arrival of the corresponding feedback signal at the atom can be estimated by considering the number of uncompensated diffusion steps m that occur during the delay time. The probability distribution over the sum of the measurement results δn accumulated within that uncontrolled interval is given by a Gaussian with a standard deviation of $\sqrt{m}|\alpha|$. This may be multiplied with the expected uncompensated diffusion step length at the stabilized point on the Bloch sphere in order to determine the reliability of feedback stabilization with a nonvanishing delay time. In the following, however, we shall concentrate on the description of effectively instantaneous feedback.

Because the total light field propagating away from the atomic system is measured in the homodyne detection, the reflected control field will also be measured in the subsequent time interval. This must be subtracted from the measurement signal for further feedback, since the feedback effect itself should not be compensated. Note that the linearity of the field dynamics involved actually allows this separation despite the fact that the feedback field and the quantum fluctuations interact with the system in a qualitatively different manner as described below. Intuitively, one would expect a complete compensation of the fluctuations if the averaged measurements of Δn are zero. However, we will see that this is not so, owing to the fact that only one quadrature of the quantum fluctuations can be compensated.

B. Effects of feedback on time scales shorter than $1/\Gamma$

Although a number of feedback scenarios may be discussed even in the simple context of the two-level atom, we will now concentrate on the possibility of stabilizing a known state with $s_y=0$ by effectively instantaneous feedback. The feedback is given by a coherent driving field inducing Rabi rotations around the s_y axis. The effect of this feedback experienced by the system during the time interval τ can be written as

$$\begin{pmatrix} \delta s_x \\ \delta s_y \\ \delta s_z \end{pmatrix}_{\text{feedback}} = 2\sqrt{\Gamma}\tau f(\Delta n) \begin{pmatrix} s_z \\ 0 \\ -s_x \end{pmatrix}, \quad (32)$$

where $f(\Delta n)$ is the feedback field describing the response of the coherent control to the most recent measurement result. Δn is the measurement result obtained from the quantum fluctuations acting on the system in the previous time interval. Since the time intervals are small on the scale of the system dynamics, however, we will simplify matters by summing the effects of the diffusion step and its subsequent feedback as if they occurred in the same time interval to obtain the effective total diffusion.

The homodyne detection measurement in the following time interval will be modified by the feedback field. The change in the Δn measurement caused by the feedback in the next measurement, δ_{next} , may be determined using Eq. (8):

$$\delta_{\text{next}} = 2|\alpha|f(\Delta n). \quad (33)$$

In order to stabilize a given system state \mathbf{s} , $f(\Delta n)$ must be chosen to compensate the diffusion step, i.e.,

$$\begin{pmatrix} \delta s_x \\ \delta s_y \\ \delta s_z \end{pmatrix}_{\text{fluctuation}} + \begin{pmatrix} \delta s_x \\ \delta s_y \\ \delta s_z \end{pmatrix}_{\text{feedback}} = 0. \quad (34)$$

For $s_y=0$, this condition is fulfilled if

$$f(\Delta n) = -(1 + \bar{s}_z) \frac{\Delta n}{2|\alpha|}, \quad (35)$$

where \bar{s}_z is the Bloch vector component of the stabilized state. Note that $f(\Delta n)$ is not a function of the present state of the atomic system.

A particularly interesting case is obtained when the feedback is chosen to compensate for the maximal fluctuation effects possible, stabilizing the excited state of the two-level atom. If the system is not in the excited state, the diffusion step associated with a homodyne detection event of Δn is now given by the sum of the original diffusion step and the feedback,

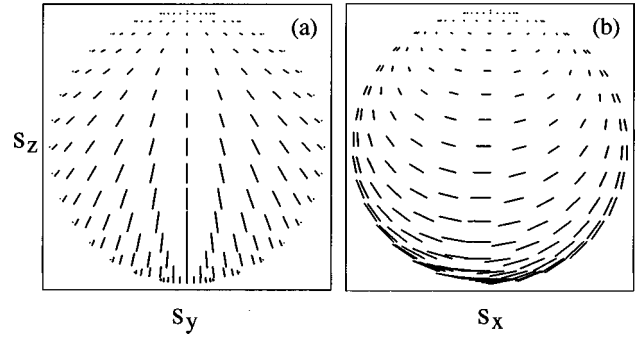


FIG. 4. Visualization of the effective diffusion step including a feedback stabilizing $\bar{s}_z = +1$. The representation is as in Fig. 1.

$$\begin{aligned} \begin{pmatrix} \delta s_x \\ \delta s_y \\ \delta s_z \end{pmatrix}_{\text{effective}} &= \sqrt{\Gamma}\tau \frac{\Delta n}{|\alpha|} \left[\begin{pmatrix} 1 + s_z - s_x^2 \\ -s_x s_y \\ -s_x(1 + s_z) \end{pmatrix} + \begin{pmatrix} -2s_z \\ 0 \\ 2s_x \end{pmatrix} \right] \\ &= \sqrt{\Gamma}\tau \frac{\Delta n}{|\alpha|} \begin{pmatrix} 1 - s_z - s_x^2 \\ -s_x s_y \\ s_x(1 - s_z) \end{pmatrix}. \end{aligned} \quad (36)$$

As shown in Fig. 4, this effective diffusion step is the exact inversion of the diffusion step without feedback. The roles of $s_z = -1$ and of $s_z = +1$ have been reversed. Consequently, the sensitivity of the system to quantum fluctuations is now maximal at the ground state, $s_z = -1$. The diffusion constant is proportional to $(1 - s_z)^2$. The in-phase quantum fluctuations have been overcompensated in this case:

$$\Delta n + \delta_{\text{next}} = -\Delta n. \quad (37)$$

This indicates that the reversal of the diffusion effect has been achieved by answering the fluctuations of the in-phase quadrature with an opposite field of double strength, effectively reversing the sign of that field component, while the unknown fluctuations in the out-of-phase quadrature are unmodified.

Another interesting scenario is the stabilization of $s_z = 0$, because it corresponds to the simple minded compensation of quantum fluctuations by choosing a feedback field with the negative amplitude of the quadrature measured in the homodyne detection. The effective diffusion step now reads

$$\begin{pmatrix} \delta s_x \\ \delta s_y \\ \delta s_z \end{pmatrix}_{\text{effective}} = \sqrt{\Gamma}\tau \frac{\Delta n}{|\alpha|} \begin{pmatrix} 1 - s_x^2 \\ -s_x s_y \\ -s_x s_z \end{pmatrix}. \quad (38)$$

As shown in Fig. 5, this diffusion law has rotational symmetry around the s_x axis. The ratio of s_y/s_z is a constant. The diffusion is always directed towards one of the two stabilized poles with $s_x = \pm 1$. The absolute value of the diffusion constant for the stabilization of $s_z = 0$ is thus given by

$$\frac{\langle \delta \mathbf{s}^2 \rangle}{\tau} = \Gamma(1 - s_x^2). \quad (39)$$

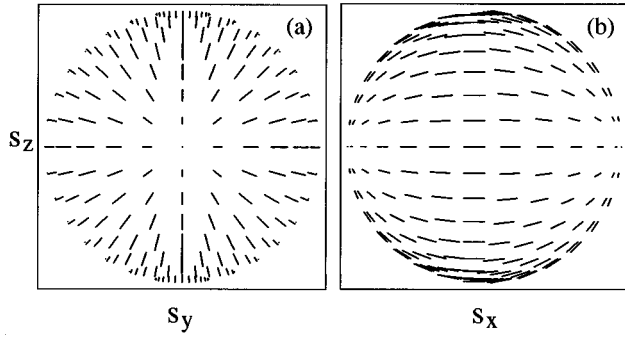


FIG. 5. Visualization of the effective diffusion step including a feedback stabilizing $\bar{s}_z=0$. The representation is as in Fig. 1.

In the general case of a stabilization of $\bar{s}_z = \cos \theta$, where θ is the angle between the stabilized Bloch vector and the s_z axis, the diffusion step is

$$\begin{pmatrix} \delta s_x \\ \delta s_y \\ \delta s_z \end{pmatrix}_{\text{effective}} = \sqrt{\Gamma \tau} \frac{\Delta n}{|\alpha|} \begin{bmatrix} s_y \\ -s_x \\ 0 \end{bmatrix} + (s_z - \cos \theta) \times \begin{pmatrix} s_z \\ 0 \\ -s_x \end{pmatrix} \quad (40)$$

and the diffusion constant is given by

$$\frac{\langle \delta \mathbf{s}^2 \rangle}{\tau} = \Gamma (1 - s_x^2 - 2(\cos \theta) s_z + \cos^2 \theta (s_x^2 + s_z^2)). \quad (41)$$

By varying the feedback it is therefore possible to suppress the diffusive dynamics for an arbitrary state in the (s_x, s_z) plane.

C. Effects of the drift terms on time scales of $1/\Gamma$

Although the feedback described above can completely suppress the random walk dynamics induced by the quantum fluctuations on a time scale of τ for an arbitrary system state, it is necessary to consider the effects of the drift terms if stability on longer time scales is to be obtained as well. The complete diffusion step, including a feedback field of $f(\Delta n) = -(1 + \cos \theta)\Delta n/2|\alpha|$, is given by

$$\begin{pmatrix} \delta s_x \\ \delta s_y \\ \delta s_z \end{pmatrix} = \begin{pmatrix} \delta s_x \\ \delta s_y \\ \delta s_z \end{pmatrix}_0 - \sqrt{\Gamma \tau} \frac{\Delta n}{|\alpha|} (1 + \cos \theta) \begin{pmatrix} s_z \\ 0 \\ -s_x \end{pmatrix}, \quad (42)$$

where $\delta \mathbf{s}_0$ denotes the diffusion step without feedback, as given by Eq. (20). The drift is consequently modified by the nonzero average of Δn in the feedback term. The resulting drift is the sum of the drift without feedback and the feedback drift term. It may be written as the sum of a rotation around the s_x axis and a rotation around the s_y axis,

$$\begin{pmatrix} \langle \delta s_x \rangle \\ \langle \delta s_y \rangle \\ \langle \delta s_z \rangle \end{pmatrix} = + \frac{\Gamma \tau}{2} (2 + s_z) s_y \begin{pmatrix} 0 \\ s_z \\ -s_y \end{pmatrix} + \frac{\Gamma \tau}{2} (s_z - 2 \cos \theta) s_x \begin{pmatrix} s_z \\ 0 \\ -s_x \end{pmatrix}. \quad (43)$$

For the stabilized state with $\bar{s}_x = \sin \theta, \bar{s}_y = 0, \bar{s}_z = \cos \theta$, the effective drift is equivalent to a Rabi rotation around the s_y axis of $(\Gamma \tau/2) \sin \theta \cos \theta$ per time interval τ . This effect can be compensated by a constant driving field. The field strength f_0 necessary for this purpose is given by

$$f_0 = \frac{\sqrt{\Gamma \tau}}{4} \sin \theta \cos \theta. \quad (44)$$

This driving field ensures that the stabilized state is a stationary solution of the drift-diffusion dynamics generated by the feedback setup. However, the drift terms may also cause problems if they amplify small deviations from this stabilized state.

The stability analysis near $s_x = \sin \theta, s_y = 0, s_z = \cos \theta$ can be performed by linearizing the drift dynamics of small deviations. The deviation in the (s_x, s_z) plane is appropriately described by the angular variable ϵ , such that $s_z = \cos(\theta + \epsilon)$ and $s_x = \sin(\theta + \epsilon)$. The linear stability analysis then shows that for small ϵ , the drift $\langle \delta \epsilon \rangle$ per time interval τ is

$$\langle \delta \epsilon \rangle = - \frac{\Gamma \tau}{2} \epsilon. \quad (45)$$

Therefore the drift terms always stabilize the state with suppressed fluctuations against rotations in the (s_x, s_z) plane. In the (s_y, s_z) plane, the situation is different however. The linearized drift dynamics of small s_y is described by

$$\langle \delta s_y \rangle = \frac{\Gamma \tau}{2} (2 + \cos \theta) (\cos \theta) s_y. \quad (46)$$

This indicates stability for all $\cos \theta < 0$, i.e., any state that has a negative s_z component. If states of higher excitation are to be stabilized, any small deviation from $s_y = 0$ in the initial preparation is amplified exponentially on a time scale of $1/\Gamma$. This indicates that long term stability of such inverted states cannot be achieved.

An interesting aspect of the quantum trajectories associated with the measurement protocols obtained from the homodyne detection is revealed in this critical problem of

quantum control. If the initial state is only known within an error margin, the trajectories may diverge and amplify this error margin even though the trajectories are fully deterministic functions of the initial state. Apparently, there is an aspect of deterministic chaos in this small quantum system when its dynamics is analyzed using homodyne detection. It seems that the fully polarized states, $s_x = \pm 1, s_y = s_z = 0$, are ideal for stabilization, since they can be observed in the measurement results. If the system drifts away from its stabilized state, this can be observed in the homodyne detection and may be corrected, either by applying static fields to shift the phase of the atomic system or by shifting the phase of the

local oscillator. In the following we will investigate the example of feedback stabilization for these maximally coherent states.

D. Stabilization of the dipole eigenstates

For $\cos \theta = 0$, the stabilized states are $s_x = \pm 1$, the eigenstates of the dipole component oscillating in phase with the local oscillator. Also, this case is special because it corresponds to the classical idea of feedback compensation: $\Delta n + \delta_{\text{next}} = 0$. At the same time, the average of Δn is a measure of s_x , indicating both the sign of the Bloch vector component stabilized and the success or failure of the stabilization attempt. The modified total diffusion step including feedback is given by

$$\begin{pmatrix} \delta s_x \\ \delta s_y \\ \delta s_z \end{pmatrix} = \sqrt{\Gamma \tau} \frac{\Delta n}{|\alpha|} \begin{pmatrix} 1 - s_x^2 \\ -s_x s_y \\ -s_x s_z \end{pmatrix} - \Gamma \tau \frac{\Delta n^2}{\alpha^* \alpha} s_x \begin{pmatrix} 1 - s_x^2 \\ -s_x s_y \\ -s_x s_z \end{pmatrix} - \Gamma \tau \frac{\Delta n^2}{\alpha^* \alpha} s_x \begin{pmatrix} s_z \\ 0 \\ -s_x \end{pmatrix} + \frac{\Gamma \tau \Delta n^2}{2 \alpha^* \alpha} (1 + s_z) \begin{pmatrix} s_x s_z \\ s_y s_z \\ s_z^2 - 1 \end{pmatrix} + \frac{\Gamma \tau}{2} \begin{pmatrix} s_x s_z \\ s_y s_z \\ s_z^2 - 1 \end{pmatrix}. \quad (47)$$

The compensation term has been split into one part that compensates the drift of the total diffusion step and the remaining term, which modifies the effective drift. The nature of the diffusion term has already been discussed in Sec. III. The diffusion steps are directed towards the s_x poles of the Bloch sphere with a diffusion constant of $\Gamma(1 - s_x^2)$. The average drift is given by

$$\begin{pmatrix} \langle \delta s_x \rangle \\ \langle \delta s_y \rangle \\ \langle \delta s_z \rangle \end{pmatrix} = + \frac{\Gamma \tau}{2} \begin{pmatrix} s_x s_z^2 \\ s_y s_z (2 + s_z) \\ -s_y^2 (2 + s_z) - s_x^2 s_z \end{pmatrix}. \quad (48)$$

Figure 6 shows the drift vectors on the Bloch sphere. The change in s_x always has the same sign as s_x , indicating that this drift will cause an increase in the dipole expectation value s_x until an eigenvector with $s_x = \pm 1$ is reached. This implies that the feedback setup actually creates the stabilized coherent state regardless of the initial state.

If the initial state is the ground state, it is sufficient to examine the drift term for $s_y = 0$, since neither the diffusion nor the drift will create an $s_y \neq 0$. The drift term is then given by

$$\begin{pmatrix} \langle \delta s_x \rangle \\ \langle \delta s_y \rangle \\ \langle \delta s_z \rangle \end{pmatrix}_{s_y=0} = + \frac{\Gamma \tau}{2} s_x s_z \begin{pmatrix} s_z \\ 0 \\ -s_y \end{pmatrix}. \quad (49)$$

This drift equation has four stationary solutions, two unstable ones at $s_z = \pm 1$, the ground state and the excited state, and two stable ones at $s_x = \pm 1$, the dipole eigenstates. Consequently the system state will be drawn towards the closest one of the two dipole eigenstates as soon as the diffusion has moved the state away from the destabilized ground state. If the phase of the local oscillator is changed, whether intentionally or accidentally, this does create an $s_y \neq 0$ compo-

nent. Since there will always be limits to the phase stability of the local oscillator, it is essential that the effects of such deviations are understood as well. For $s_z = 0$, the system reacts with a diffusion in the (s_x, s_y) plane and a drift reducing s_z . For small values of s_y , the system will relax exponentially to $s_z = -2s_y^2$. This induces a drift in s_y corresponding to

$$\frac{d}{dt} s_y = -2\Gamma s_y^3. \quad (50)$$

This stabilization of $s_y = 0$ is very weak compared to the exponential stability in $s_z = 0$. The dynamics of the relaxation for small deviations is approximately given by

$$s_y(t) = \frac{1}{\sqrt{4\Gamma t + [s_y(0)]^{-2}}}. \quad (51)$$

Figure 7 shows a comparison of this relaxation with the exponential relaxation of s_z . This comparison clearly demonstrates that the relaxation of s_y may indeed be separated from the fast relaxation of s_z . Note that since the relaxation of s_y is very slow, its effect cannot be separated from the diffusion. The diffusion constant of Γs_y^2 is actually quite similar to the drift term of s_y . Consequently, the trajectory of the system dynamics will be more complicated and unpredictable than suggested by Eq. (51) and Fig. 7.

On time scales longer than $1/\Gamma$, the expectation value of the dipole variable s_x can be observed in the averages of Δn . This may serve as a control of the stabilization process and possibly as an additional tool to produce the correct phase relation between the local oscillator and the atomic system. Note that it is fairly safe to interpret small deviations from $s_x = \pm 1$ as phase mismatches between the local oscillator

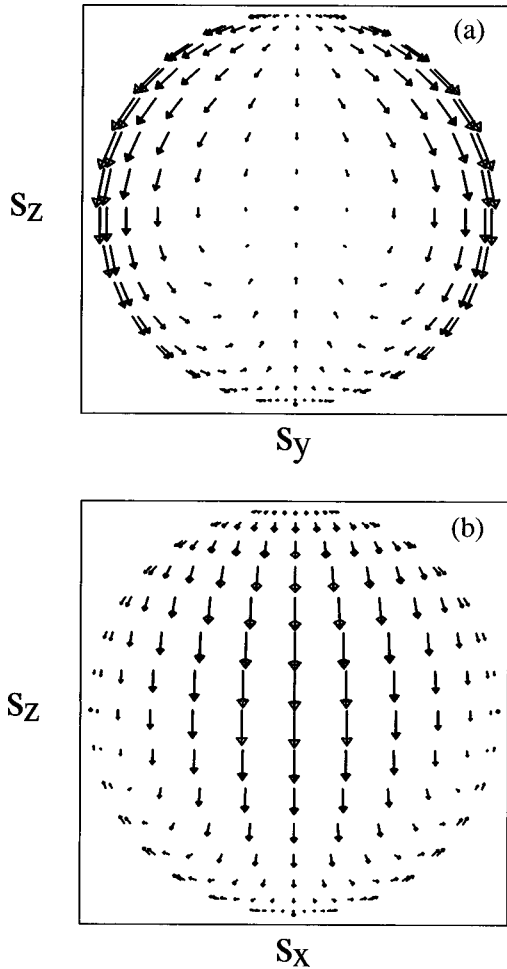


FIG. 6. Effective drift on the Bloch sphere including a feedback stabilizing $\bar{s}_z=0$. (a) shows the projection into the (s_y, s_z) plane and (b) the projection into the (s_x, s_z) plane.

and the atomic system since the phase stability given by s_y is so much weaker than the excitation stability given by s_z .

E. Implications for coupled and multilevel atomic systems

The major part of this paper is concerned with the possibility of observing and manipulating the dynamics of a simple atomic two-state system interacting with the light field continuum. The theory of photon emission used may also be extended to coupled and multilevel systems, as shown in [10] for a simple quantum beat scenario. One important aspect of the effects of homodyne detection of light field emissions from larger electronic systems, such as networks of coupled quantum dots, is that the contribution of the system dynamics must be considered in more detail. In fact, the presence of different frequencies in the system dynamics may effectively remove the difference between homodyne and heterodyne detection. In quantum beat scenarios such as the ones considered in [10,16], the homodyne detection could be performed on only one of the emission channels, with consequences for the probability of detecting an emission in the other channel. If the coupling strength of the transitions is very different [16], the quantum fluctuations coupling to the fast transitions will induce phase fluctuations in the dynamics of the system. Such phase fluctuations in the

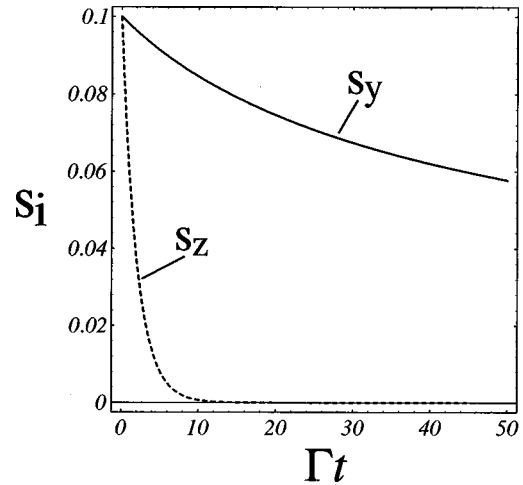


FIG. 7. Comparison of the approximate relaxation dynamics of $s_z(0)=0.1$ and $s_y(0)=0.1$ in the presence of a feedback stabilizing $\bar{s}_z=0$. s_y does not change much while the exponential relaxation effectively reduces s_z to zero.

quantum beats of a system could be measured by homodyne detection. The resulting correlation between the measurement protocols of the homodyne detection and the probability of an emission from a local part of the system can be predicted using quantum trajectory formalisms such as the one presented in this paper. The effective projective measurement base of an eight port homodyne detection, which was discussed in [4], may also be applied in place of the simple balanced homodyne detection scheme used here. This would restore the symmetry between s_x and s_y , increasing the number of possible stabilization scenarios.

V. INTERPRETATION AND CONCLUSIONS

A. Interpretation of the light-atom interaction

In the usual photon detection measurement the quantum fluctuations of the vacuum field state seem to have no effect. This impression is a result of the particle picture interpretation associated with the photon measurement. If homodyne detection is used instead, the information obtained is mainly information about the quantum fluctuations acting on the system, with only small contributions from the in-phase dipole component of the atomic system. While the information about the time of photon emission is lost completely, the evolution of the atomic dipole oscillations may be reconstructed from the measurement protocols.

However, the Bloch vector does not react to the quantum fluctuations in the same way as it would respond to a classical driving field. The fact that no energy may be absorbed from the quantum fluctuations of the light field vacuum requires that the ground state is not influenced by the fluctuations. At the same time, the corresponding excited state is much more sensitive to the fluctuations. This asymmetry required by energy conservation may also be understood in terms of a correlation of the atomic system and the field. The atomic ground state is really a dressed state in which the field and dipole fluctuations are correlated so as to preserve the state of lowest energy. Consequently, there is a similar correlation in the excited state, which enhances the interaction with the quantum fluctuations. Of course, this correlation

extends only to the quantum noise. Therefore, the coherent fields used to control the atom interact in a different manner and can never compensate the dissipative effects. This can only be achieved by manipulating the electromagnetic vacuum itself, for example, by putting the atom into a microcavity.

The peculiar nature of quantum states and quantum-mechanical uncertainty is also apparent in the asymmetry of the diffusion step. If the quantum state is considered to be an objectively real description of the atomic system it is difficult to explain the dependence of the diffusion step on the phase of the local oscillator used in the homodyne detection, especially since the measurement could be performed a long time after the emission and at an arbitrary distance. Thus this simple balanced homodyne detection scenario also highlights the epistemological nature of the wave function and the resulting nonlocality.

The analysis of the contributions to the spontaneous emission process observed on time scales of $1/\Gamma$ reveals a surprisingly complex structure of the process, with contributions from quasiclassical dipole radiation and nonlinear effects of the fluctuations. The interpretation of these terms is far from complete and reveals new challenges to our physical understanding presented by this fundamental quantum-mechanical process.

B. Conclusions

We have presented a completely quantum-mechanical theory of homodyne detection, simulating the time-resolved observation of electromagnetic emissions from an atomic system at a quantum efficiency of 100%. The theory includes a model of the unitary evolution of the system-field correlation and applies projective measurements to the results of this temporal evolution. The information obtained about the dissipative dynamics of the atomic system has been applied in feedback scenarios which demonstrate that the dissipative dynamics can be modified by feedback to create and stabilize excited or coherent states of the system. The dissipative nature of the measurement cannot be compensated however, and excited states show an instability with regard to small errors in the initial preparation on time scales of $1/\Gamma$, the natural lifetime of the excited state. In conclusion, we have shown that homodyne detection can be a useful tool in attempts to observe and control individual quantum systems.

ACKNOWLEDGMENTS

We would like to thank Ariel Liebmann and Claus Granzow for many helpful discussions, and Howard Carmichael for valuable comments.

-
- [1] H. P. Yuen and J. H. Shapiro, in *Coherence and Quantum Optics IV*, edited by L. Mandel and E. Wolf (Plenum, New York, 1978), p. 719.
 - [2] S. L. Braunstein, *Phys. Rev. A* **42**, 474 (1990).
 - [3] W. Vogel and J. Grabow, *Phys. Rev. A* **47**, 4227 (1993).
 - [4] A. Luis and J. Perina, *Quantum Semiclassic. Opt.* **8**, 873 (1996).
 - [5] H. Carmichael, *An Open Systems Approach to Quantum Mechanics* (Springer, Berlin, 1993).
 - [6] H. M. Wiseman and G. J. Milburn, *Phys. Rev. A* **47**, 642 (1993).
 - [7] H. M. Wiseman, *Quantum Semiclassic. Opt.* **8**, 205 (1996).
 - [8] H. M. Wiseman and G. J. Milburn, *Phys. Rev. Lett.* **70**, 548 (1993).
 - [9] H. M. Wiseman, *Phys. Rev. A* **49**, 2133 (1994).
 - [10] H. F. Hofmann and G. Mahler, *Quantum Semiclassic. Opt.* **7**, 489 (1995).
 - [11] A. Einstein, R. C. Tolman, and B. Podolski, *Phys. Rev.* **37**, 780 (1931); *Quantum Theory and Measurement*, edited by J. A. Wheeler and W. H. Zurek (Princeton University Press, Princeton, 1983), p. 135.
 - [12] R. H. Dicke, *Phys. Rev.* **93**, 99 (1954).
 - [13] R. Bonifacio, P. Schwendimann, and F. Haake, *Phys. Rev. A* **4**, 302 (1971).
 - [14] C. Gerthsen, H. O. Kneser, and H. Vogel, *Physik* (Springer, Berlin, 1986), p. 844.
 - [15] M. Ueda and M. Kitagawa, *Phys. Rev. Lett.* **68**, 3424 (1992).
 - [16] H. F. Hofmann, in *Quantum Coherence and Decoherence*, edited by K. Fujikawa and Y. A. Ono (Elsevier, New York, 1996), p. 39.